One-step electrodeposition of ligand-free PdPt alloy nanoparticles from water droplets: Controlling size, coverage, and elemental stoichiometry

Andrew Pendergast, Matthew Glasscott, Christophe Renault, Jeffrey Dick

One-Step Electrodeposition of PdPt Alloy Nanoparticles from Water Droplets: Controlling Size, Coverage, and Elemental Stoichiometry

Andrew D. Pendergast[a], Matthew W. Glasscott[a], Christophe Renault,[b] and Jeffrey E. Dick*[,a]

[a]Department of Chemistry, The University of North Carolina at Chapel Hill, Chapel Hill, NC 27599

[b]Physique de la Matière Condensée, CNRS, Ecole Polytechnique, 91128 Palaiseau, France

*To whom correspondence should be address: jedick@email.unc.edu

Abstract:

We present a robust and facile method to produce metal nanoparticle (NP) alloys in a one-step synthesis using direct electrodeposition onto highly oriented pyrolytic graphite (HOPG). Precursor salts, H_2PtCl_6 and $Pd(NO_3)_2$, were dissolved in a 1 mM sodium dodecylsulfate (SDS) water droplet with 1X phosphate buffered saline solution and suspended in a dichloroethane (DCE) continuous phase. Tetrabutylammonium perchlorate was added to the DCE continuous phase to maintain charge balance during electrodeposition. NP fabrication *via* electrodeposition was driven by droplet collisions onto HOPG, which was biased at a potential where the metal precursor salts would reduce to their respective zero-valent atoms. Scanning Electron Microscopy (SEM) and Energy Dispersive X-Ray Spectroscopy (EDX) were used to study the size, coverage, and morphology of the NPs as well as the atomic stoichiometry. EDX mapping indicated homogeneous distribution of Pd and Pt at the single NP level. Homogeneously alloyed PdPt NPs were realized from this study with demonstrated control over metal composition, surface coverage, and NP size.

Key Words: Alloy, Nanoparticle, Bimetallic, Emulsion Droplet, Electrodeposition

1. Introduction

Owing to their unique chemical and physical properties that sometimes differ from bulk, polycrystalline metals, metallic nanoparticles (NPs) have received extensive interest in the field of electrochemistry with a particular emphasis on electrocatalysis and sensing applications [1-5]. Previous articles have reported metal nanoparticle collision events at ultramicroelectrodes to study fundamental electrochemical processes at the single NP level with applications towards understanding electrocatalytic activity at the nanoscale [3, 6]. Sometimes, however, NPs made of a single metal do not present desired stability or activity. For electrocatalysis in particular, metal alloy NPs (MANPs) offer tremendous advantages over single metal NPs in their chemical and physical properties [7, 8]. For instance, direct methanol oxidation on platinum is difficult due to the deleterious effects of carbon monoxide poisoning; however, it has been shown that the incorporation of palladium into platinum allows for effective methanol oxidation without the poisoning effects of carbon monoxide [9-11]. Furthermore, the addition of iron oxide into a nickel oxide electrocatalyst has been shown to greatly increase the activity toward the oxygen evolution reaction [12]. Beyond electrocatalytic applications, bimetallic and higher-order alloyed NPs can offer unique structural, magnetic, and optical properties compared to monometallic and bulk materials [13]. Importantly, the structure and elemental composition of homogeneous NPs can be modified to optimize catalytic pathways by combining unary elemental properties and revealing novel dynamic properties [14, 15]. Thus, the ability to alloy metal NPs and control the stoichiometry is of great importance.

To study the electrochemical properties of MANPs, the general requirement of attaching the MANPs to a substrate must be met for measurements to be made. While success has been made in the homogeneous synthesis of MANPs and subsequent adsorption of MANPs onto conductive

surfaces [13], these MANPs must incorporate a ligand to achieve a stable colloidal suspension. Previously, Booth and co-workers used an electron-transfer mediator to generate gold NPs at the interface between a trifluorotoluene droplet and water, effectively producing a Pickering emulsion droplet [16]. From these experiments, two main limitations must be considered: 1.) The use of ligands may block surface sites for electrocatalytic reactions, impeding the study of NP reactivity [17-21] and 2.) drop-casting and adsorption onto a substrate does not guarantee electrical connection of the MANP to the underlying substrate, thereby leading to variability in the total charge transfer observed *via* electrochemical characterization [22]. One method of solving these issues is by direct electrodeposition of MANPs onto the surface of an electrode. Direct electrodeposition does not require stabilizing ligands, maximizing the surface area of a MANP available for electrocatalytic studies. Electrodeposition also requires contact to be made to the underlying substrate, such as highly-oriented pyrolytic graphite (HOPG) [23]**,** minimizing the fraction of MANPs without electrical contact. Previous efforts have suggested that emulsion-based systems can be used to generate NPs by direct electrodeposition [24], however, these techniques demonstrate limited control over NP size, morphology, and coverage.

Classical electrodeposition of MANPs is not well characterized due to difficulties in controlling size, coverage, morphology, and composition of the NPs. We recently addressed the issue of non-homogeneous electrodeposition of metal NPs with a new method. This method is based on the electrodeposition of monometallic NPs from aqueous droplets suspended in a dichloroethane (DCE) phase (i.e. a water-in-oil emulsion). Briefly, a metal precursor confined in a water droplet is reduced to metal when the freely diffusing droplet collides with the surface of a conducting substrate biased at a sufficiently cathodic potential for electrodeposition to occur. We assume that each droplet collision results in the electrodeposition of a metal NP, which was

supported by an analysis of the mass transfer of droplets [25]. The stochastic nature of the collision generates a random distribution of NPs on the surface. We have demonstrated accurate control over surface coverage and size for Pt NPs deposited on amorphous graphitic substrates [25, 26]. Our approach was also extended to the electrodeposition of Au, Ag, Sn, Ce, Fe, and Cu NPs onto various substrates including boron-doped diamond, gold, silicon, and highly oriented HOPG. Here, we extend this method to the electrosynthesis of PdPt MANPs and demonstrate control over size, coverage on HOPG, and stoichiometric composition of metals. This method represents the first of its kind to robustly control size, coverage, and metal composition during electrodeposition experiments.

2. Experimental

All chemical reagents were analytic grade and used without further purification. Stock solutions of each metal (100-300 mM) were made in MilliQ water (>18.2 MΩ•cm) and diluted as necessary to be used in the emulsion preparation. It is important to note that metal salt precursor stock solutions can photodegrade under ambient conditions, therefore a fresh stock solution should be made for daily experiments. The electrodeposition experiments were performed using a CHI model 601E potentiostat (CH Instruments, Austin, TX) on the "Amperometric i-t curve" mode. Scanning Electron Microscopy (SEM) images and Energy Dispersive X-Ray Spectroscopy (EDX) spectra were taken using a Helios 600 Nanolab Dual Beam System (FEI, Hillsboro, OR) and INCA PentaFET -x3 (Oxford, Abingdon, United Kingdom) respectively at 30 keV and 0.69 nA. A schematic diagram of the NP electrodeposition procedure is presented in Figure 1.

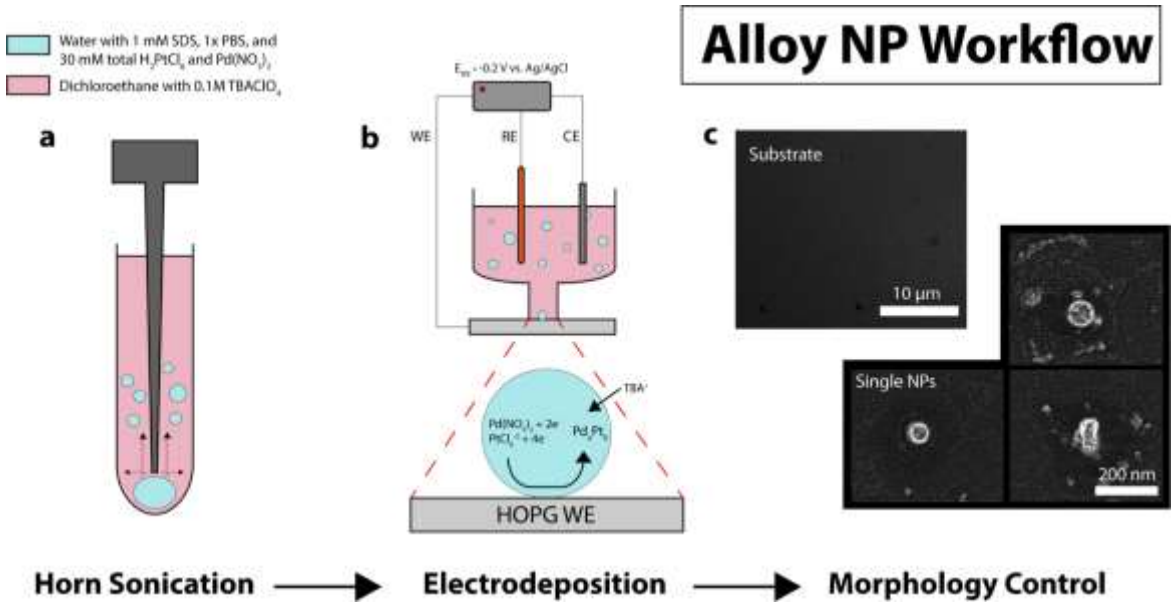

Figure 1. a) A water-in-DCE emulsion was prepared by horn sonication, b) following ultrasonication, droplet-mediated electrodeposition occurs at the droplet-electrode interface, c) Surface coverage and NP size were controlled by electrodeposition time and metal salt precursor concentration respectively. SEM images on the right show a representative HOPG substrate following electrodeposition of $Pd_{0.5}Pt_{0.5}$ NPs and representative single NP morphologies.

First, a water-in-DCE emulsion was prepared from a 30 µL 1 mM sodium dodecylsulfate (SDS) aqueous droplet containing 15 mM H_2PtCl_6 and 15 mM $Pd(NO_3)_2$ and 1X phosphate buffered saline solution (PBS), in an organic phase of 5 mL DCE with 0.1 M tetrabutlyammonium perchlorate ($TBAClO_4$). $TBAClO_4$ was used as a non-aqueous supporting electrolyte necessary to maintain charge balance during the electrodeposition by the transfer of TBA+ across the oil|water interface [27]. Three different emulsions were prepared to demonstrate stoichiometric control: $Pd_{0.1}Pt_{0.9}$, $Pd_{0.5}Pt_{0.5}$, and $Pd_{0.9}Pt_{0.1}$. Emulsions were formed by ultrasonication (500 W, amplitude 40%, 1/16th" microtip probe, Q500 Ultrasonic Processor, Qsonica, CT) with a pulsed sonication method (5 s on, 5 s off; total 6 cycles). A HOPG substrate with an exposed radius of 2 mm (the working electrode, WE in Figure 1) is biased at -0.2 V vs Ag/AgCl (1M KCl quasi reference electrode, RE in Figure 1) [25, 28], a sufficiently negative potential to ensure the reduction of both metal salts as depicted in the schematic zoom of a single droplet in Figure 1.

We found that -0.2 V was sufficient enough for electrodeposition due to the manifestation of NPs in electron micrographs. The counter electrode (CE in Figure 1) is a Pt wire. The cell is filled with 2.0 mL of emulsion solution, and a chronoamperogram was recorded. After electrodeposition over typically 1000 s, the substrate is rinsed with DCE, 100% ethanol, and MilliQ water for 5 minutes each to remove residual salts and surfactants. A UV-Vis analysis indicated up to 1.6% of metal salt partitioned out of the droplets due to the sonication process (data not shown). While this small amount of salt had no negative effects on NP electrosynthesis, the effects of metal ion partitioning at the water-DCE interface on NP structure is currently being investigated.

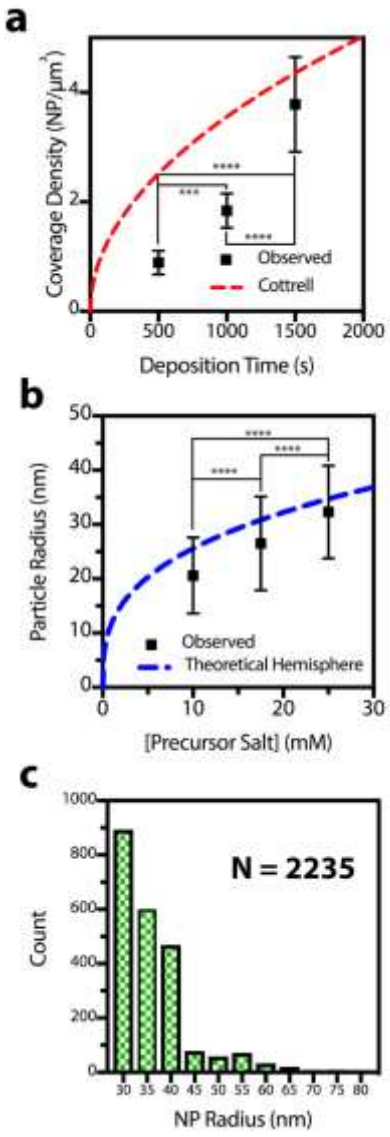

Figure 2. a) Substrate coverage by PdPt NPs (30 mM total metal salt precursor) can be controlled by tuning electrodeposition time. b) $Pd_{0.5}Pt_{0.5}$ NP size can be modulated by varying total metal precursor ion concentration in aqueous droplet. c) 30 mM $Pd_{0.5}Pt_{0.5}$ NP population radius distribution following 1000s deposition.

3. Results and Discussion

3.1 Size and Coverage Control

A representative SEM image of a HOPG substrate following PdPt alloy NP electrodeposition is shown in Figure 1c with bright spots corresponding to NPs. Under our experimental conditions, the surface density of NPs is homogeneous as previously shown for monometallic NPs electrodeposited using this method [25]. The NP density on the underlying substrate can be adjusted by varying electrodeposition time. Figure 2a evidences that the coverage of NP varies with the duration of electrodeposition, as expected for a system where

the arrival of droplets at the substrate is controlled by semi-infinite linear diffusion. The red line is a theoretical model of the integrated form of the Cottrell equation for the conditions of electrodeposition normalized to area, calculated from the following equation:

$$\textbf{Coverage}\left(\frac{NPs}{m^2}\right) = 2C^* D^{\frac{1}{2}} \pi^{-\frac{1}{2}} t^{\frac{1}{2}} N_A \qquad \textbf{Equation 1 [25, 29]}$$

where C is the concentration of droplets, D is the diffusion coefficient of droplets, t is time, and N_A is Avogadro's number. Here, the diffusion coefficient of a droplet is estimated using the Stokes-Einstein approximation. The observed deviation from Cottrellian behavior may be explained by the presence of droplet stabilizing surfactant which can inhibit electron transfer at the droplet-electrode interface coupled with polydispersity in the emulsion droplet size [26]. Understanding the underlying complex NP electrodeposition and precursor ion diffusion mechanisms is a current avenue of study in this lab.

Representative NP micrographs are additionally presented in Figure 1c demonstrating unique morphologies *via* electrodeposition. The average radius of the NPs is 32 ± 8 nm with a hemispherical morphology with a size distribution as presented in Figure 2c. The size of the NP can be tuned by changing the concentration of metal precursor inside the droplets. Figure 2b shows statistically significant variations in mean NP radius from 20 to 30 nm when changing the total metal precursor concentration from 10 to 25 mM (statistical analysis *via* One-Way ANOVA with Turkey's t-test for multiple comparisons). The relationship between initial precursor concentration in the droplet and NP radius follows a cubic root law (see blue line in Figure 2b). The volume, and thus the size, of the resulting NP is found by multiplying the volume of the unit cell by the total number of unit cells, assuming that each molecule of precursor salt reduces to a single metal atom in a fcc lattice.

3.2 Stoichiometric Control

We were interested in determining whether or not the electrodeposited NPs are an alloy of Pt and Pd or two separated phases. Representative SEM and EDX images are shown in Figure 3 for the three different molar ratios of Pt and Pd salt precursors (final concentration 50 mM). SEM images of individual NPs with molar ratios of $Pd_{0.1}Pt_{0.9}$, $Pd_{0.5}Pt_{0.5}$, and $Pd_{0.9}Pt_{0.1}$ present similar morphologies and rough surfaces. Elemental mapping of Pt and Pd on individual NPs evidences a homogeneous distribution of the metals within the NP and an overlap throughout the domain of a single NP. This observation clearly differs from intermetallic microstructure characteristic of core shell particles that have previously been reported [11, 30]. EDX analysis for molar ratio determination was conducted on NPs with radii up to approximately 100 nm, however, elemental mapping on smaller NPs significantly reduced micrograph resolution due to instrumental drift over long exposure integration times. The Pt and Pd mapping was used to semi-quantitatively analyze the atomic composition of a single NP. Alloy NPs made from droplets containing a molar ratio of $Pd_{0.1}Pt_{0.9}$, $Pd_{0.5}Pt_{0.5}$, and $Pd_{0.9}Pt_{0.1}$ present atomic ratios of $Pd_{0.89}Pt_{0.11}$,

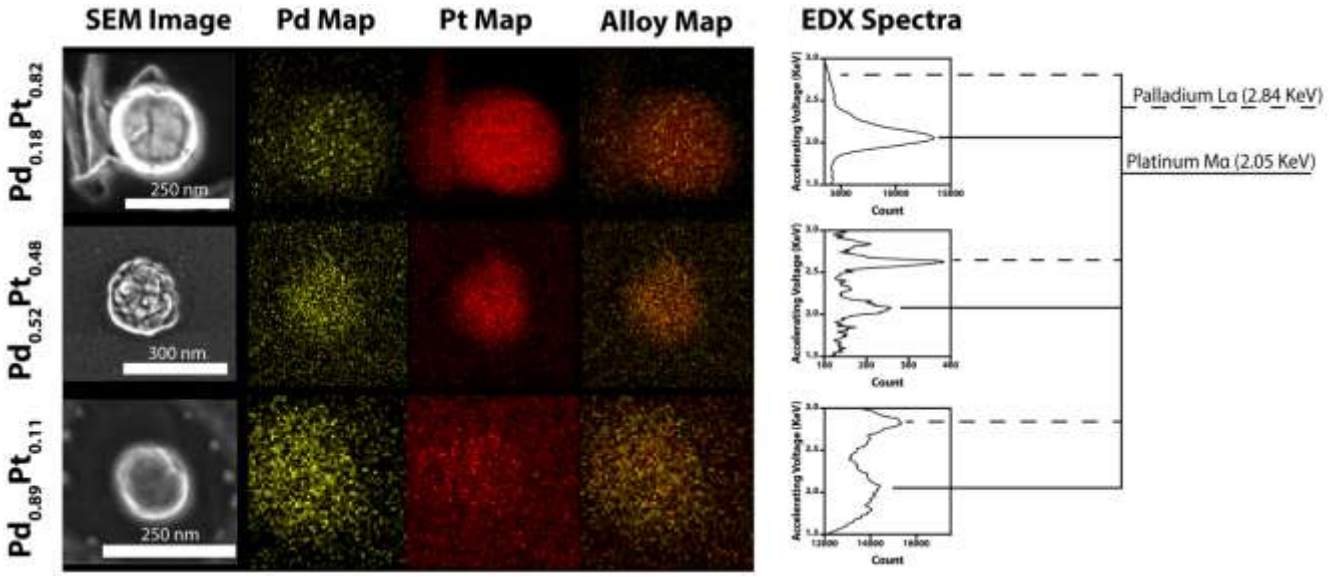

Figure 3. Representative SEM images, EDX elemental maps, and EDX spectra of varying stoichiometry Pd_xPt_y NPs demonstrating consistent elemental homogeneity independent of precursor ion concentration. Representative EDX spectra presented with highlighted characteristic Pd Lα X-ray peak at 2.84 KeV and Pt Mα X-ray peak at 2.05 KeV. EDX elemental map brightness has been normalized according to theoretical stoichiometry.

$Pd_{0.52}Pt_{0.48}$, and $Pd_{0.18}Pt_{0.82}$ respectively. The $Pd_{0.89}Pt_{0.11}$and $Pd_{0.52}Pt_{0.48}$ molar ratio follow closely the initial ratio of precursors inside the droplet. The minor deviation observed for the $Pd_{0.1}Pt_{0.9}$ case can possibly be attributed to uncertainties in the quantification. Most importantly, the composition of the alloy can be conveniently tuned by adjusting the initial relative concentration of precursors inside the droplet. The mechanism of NP formation within the droplet is currently under investigation. As elemental stoichiometry has been previously shown to enhance electrocatalytic properties of alloyed materials above monometallic metal systems, NP electrocatalytic characterization via voltammetry is a current investigation of this laboratory.

Conclusion

In conclusion, we demonstrate that electrodeposition of NPs via co-reduction of $PtCl_6^{-2}$ and $Pd(NO_3)_2$ in a water-in-oil emulsion system generates alloyed NPs with tuneable stoichiometry. Fabrication of these alloy NPs can be controlled with respect to NP size and substrate coverage. While a number of NP fabrication techniques currently exist, this proposed droplet deposition technique offers a novel method to generate alloy NPs. This approach enables homogeneous functionalization of any conducting substrate with alloy NPs and in principle can be extended to any alloy provided metal precursors are stable in water and can be electrochemically reduced. The flexibility of our electrodeposition technique coupled with the numerous interesting properties of alloys renders this technique desirable for a wide range of applications.

Conflict of Interest Statement

Declarations of interest: none.

Acknowledgements

We would like to acknowledge the University of North Carolina at Chapel Hill for start-up funds, which supported this work. This work was performed in part at the Chapel Hill Analytical and Nanofabrication Laboratory, CHANL, a member of the North Carolina Research Triangle Nanotechnology Network, RTNN, which is supported by the National Science Foundation, Grant ECCS-1542015, as part of the National Nanotechnology Coordinated Infrastructure, NNCI. C.R. acknowledges the funding of the CNRS and the Agence Nationale de la Recherche (ANR-17-CE09-0034-01, "SEE").

References

[1] L. Rassaei, F. Marken, M. Sillanpää, M. Amiri, C.M. Cirtiu, M. Sillanpää, Nanoparticles in electrochemical sensors for environmental monitoring, TrAC Trends in Analytical Chemistry, 30 (2011) 1704-1715.
[2] R.M. Penner, Electrodeposited nanophotonics, The Journal of Physical Chemistry C, 118 (2014) 17179-17192.
[3] T.R. Bartlett, J. Holter, N. Young, R.G. Compton, Nanoelectrode array formation by electrolytic nanoparticle impacts, Nanoscale, 8 (2016) 13908-13914.
[4] K.J. Stevenson, K. Tschulik, A materials driven approach for understanding single entity nano impact electrochemistry, Current Opinion in Electrochemistry, 6 (2017) 38-45.
[5] L.K. Allerston, N.V. Rees, Nanoparticle impacts in innovative electrochemistry, Current Opinion in Electrochemistry, 10 (2018) 31-36.
[6] S.V. Sokolov, S. Eloul, E. Kätelhön, C. Batchelor-McAuley, R.G. Compton, Electrode–particle impacts: a users guide, Physical Chemistry Chemical Physics, 19 (2017) 28-43.
[7] C. Chen, Y. Kang, Z. Huo, Z. Zhu, W. Huang, H.L. Xin, J.D. Snyder, D. Li, J.A. Herron, M. Mavrikakis, M. Chi, K.L. More, Y. Li, N.M. Markovic, G.A. Somorjai, P. Yang, V.R. Stamenkovic, Highly crystalline multimetallic nanoframes with three-dimensional electrocatalytic surfaces, Science, 343 (2014) 1339-1343.
[8] P. Qiao, S. Zou, S. Xu, J. Liu, Y. Li, G. Ma, L. Xiao, H. Lou, J. Fan, A general synthesis strategy of multi-metallic nanoparticles within mesoporous titania via in situ photo-deposition, Journal of Materials Chemistry A, 2 (2014) 17321-17328.
[9] W. He, H. Jiang, Y. Zhou, S. Yang, X. Xue, Z. Zou, X. Zhang, D.L. Akins, H. Yang, An efficient reduction route for the production of Pd–Pt nanoparticles anchored on graphene nanosheets for use as durable oxygen reduction electrocatalysts, Carbon, 50 (2012) 265-274.
[10] Y. Liu, M. Chi, V. Mazumder, K.L. More, S. Soled, J.D. Henao, S. Sun, Composition-controlled synthesis of bimetallic PdPt nanoparticles and their electro-oxidation of methanol, Chemistry of Materials, 23 (2011) 4199-4203.
[11] L. Wang, Y. Yamauchi, Strategic Synthesis of trimetallic Au@Pd@Pt core–shell nanoparticles from poly(vinylpyrrolidone)-based aqueous solution toward highly active electrocatalysts, Chemistry of Materials, 23 (2011) 2457-2465.
[12] J.M. Barforoush, T.E. Seuferling, D.T. Jantz, K.R. Song, K.C. Leonard, Insights into the active electrocatalytic areas of layered double hydroxide and amorphous nickel–iron oxide oxygen evolution electrocatalysts, ACS Applied Energy Materials, 1 (2018) 1415-1423.
[13] R. Ferrando, J. Jellinek, R.L. Johnston, Nanoalloys: from theory to applications of alloy clusters and nanoparticles, Chemical Reviews, 108 (2008) 845-910.
[14] S.E.F. Kleijn, S.C.S. Lai, M.T.M. Koper, P.R. Unwin, Electrochemistry of nanoparticles, Angewandte Chemie International Edition, 53 (2014) 3558-3586.
[15] P.-C. Chen, X. Liu, J.L. Hedrick, Z. Xie, S. Wang, Q.-Y. Lin, M.C. Hersam, V.P. Dravid, C.A. Mirkin, Polyelemental nanoparticle libraries, Science, 352 (2016) 1565-1569.
[16] S.G. Booth, R.G. Alghamdi, D. Belić, M. Brust, Electrodeposition of gold nanostructures at the Interface of a Pickering emulsion, ChemElectroChem, 5 (2018) 2055-2058.

[17] X. Xiao, A.J. Bard, Observing single nanoparticle collisions at an ultramicroelectrode by electrocatalytic amplification, Journal of the American Chemical Society, 129 (2007) 9610-9612.
[18] F.-R.F. Fan, A.J. Bard, Observing single nanoparticle collisions by electrogenerated chemiluminescence amplification, Nano Letters, 8 (2008) 1746-1749.
[19] H. Zhou, F.-R.F. Fan, A.J. Bard, Observation of discrete Au nanoparticle collisions by Eeectrocatalytic amplification using Pt ultramicroelectrode surface modification, The Journal of Physical Chemistry Letters, 1 (2010) 2671-2674.
[20] J.E. Dick, A.J. Bard, Toward the digital electrochemical recognition of cobalt, iridium, nickel, and iron ion collisions by catalytic amplification, Journal of the American Chemical Society, 138 (2016) 8446-8452.
[21] S.J. Percival, B. Zhang, Fast-scan cyclic voltammetry allows determination of electron-transfer kinetic constants in single nanoparticle collision, The Journal of Physical Chemistry C, 120 (2016) 20536-20546.
[22] A.J. Wilson, K. Marchuk, K.A. Willets, Imaging electrogenerated chemiluminescence at single gold nanowire electrodes, Nano Letters, 15 (2015) 6110-6115.
[23] G. Zhang, A.S. Cuharuc, A.G. Güell, P.R. Unwin, Electrochemistry at highly oriented pyrolytic graphite (HOPG): lower limit for the kinetics of outer-sphere redox processes and general implications for electron transfer models, Physical Chemistry Chemical Physics, 17 (2015) 11827-11838.
[24] Y.E. Jeun, B. Baek, M.W. Lee, H.S. Ahn, Surfactant-free electrochemical synthesis of metallic nanoparticles via stochastic collisions of aqueous nanodroplet reactors, Chemical Communications, 54 (2018) 10052-10055.
[25] M.W. Glasscott, A.D. Pendergast, J.E. Dick, A universal platform for the electrodeposition of ligand-free metal nanoparticles from a water-in-oil emulsionsSystem, ACS Applied Nano Materials, (2018).
[26] M.W. Glasscott, J.E. Dick, Direct Eeectrochemical observation of single platinum cluster electrocatalysis on ultramicroelectrodes, Analytical Chemistry, 90 (2018) 7804-7808.
[27] A. L. Barker, P. Unwin, Measurement of solute partitioning across liquid/liquid interfaces using scanning electrochemical microscopy−double potential step chronoamperometry (SECM−DPSC): principles, theory, and application to ferrocenium ion transfer across the 1,2-dichloroethane/aqueous interface, Journal of of Physical Chemistry B, 105 (2001) 12019-12031.
[28] G.A. East, M.A. del Valle, Easy-to-make Ag/AgCl reference electrode, Journal of Chemical Education, 77 (2000) p.97.
[29] A.J.F. Bard, Larry R. , Electrochemical methods: fundamentals and applications, 2nd Edition, Wiley, 2000.
[30] V. Mazumder, M. Chi, K.L. More, S. Sun, Core/shell Pd/FePt nanoparticles as an active and durable catalyst for the oxygen reduction reaction, Journal of the American Chemical Society, 132 (2010) 7848-7849.